World Academy of Science, Engineering and Technology
International Journal of Bioengineering and Life Sciences
Vol:17, No:5, 2023

Recognition of Gene Names from Gene Pathway Figures Using Siamese Network

Muhammad Azam, Micheal Olaolu Arowolo, Fei He, Mihail Popescu, Dong Xu

***Abstract*—**The number of biological papers is growing quickly, which means that the number of biological pathway figures in those papers is also increasing quickly. Each pathway figure shows extensive biological information, like the names of genes and how the genes are related. However, manually annotating pathway figures takes a lot of time and work. Even though using advanced image understanding models could speed up the process of curation, these models still need to be made more accurate. To improve gene name recognition from pathway figures, we applied a Siamese network to map image segments to a library of pictures containing known genes in a similar way to person recognition from photos in many photo applications. We used a triple loss function and a triplet spatial pyramid pooling network by combining the triplet convolution neural network and the spatial pyramid pooling (TSPP-Net). We compared VGG19 and VGG16 as the Siamese network model. VGG16 achieved better performance with an accuracy of 93%, which is much higher than Optical Character Recognition (OCR) results.

***Keywords*—**Biological pathway, image understanding, gene name recognition, object detection, Siamese network, Visual Geometry Group.

I. Introduction

IN academic articles, biological pathway diagrams depict the biological functions and processes, which typically include multiple genes and their interactions. For biological investigations and subsequent applications, the gene names and their relationships in route diagrams are excellent tools. The number of pathway diagrams rises quickly along with the biological literature. The exponential increase in publications makes it impossible for manual curation of gene names and their correlations in pathway figures to stay up. Therefore, it is necessary to automate information extraction from pathway diagrams to reduce the labor-intensive human curation needed to identify both gene names and gene connections in the figures [1]. One can use OCR tools to recognize gene names in figures, but the accuracies are limited. Reference [2] formulated an image recognition problem, i.e., to map a query image containing a gene name to a library of pictures containing known genes, in a similar way like person recognition from photos in photo applications.

In the last several years, deep learning techniques have often been increasingly applied to solve a broad range of problems. Convolutional neural networks (CNN) are particularly good at a range of computer vision tasks, including semantic segmentation [3], object identification [4], image retrieval, and image categorization. Deep architectures make it easier to learn semantic abstractions like those used in human cognition. According to recent research, CNN features may be applied to various datasets like ImageNet [5]. CNN variants such as Alex Net [6], VGGNet [7], and GoogLetNet [8] have also demonstrated successes.

Modern methods for learning feature similarity include Siamese and triplet networks [9]. These networks utilize two or three identical CNN branches and change the weights to provide a high-level representation of images (or other types of samples). Similar image pairings are mapped close together in the feature space, while dissimilar image pairs are mapped far apart. Specifically, the triplet network is recognized as an advanced approach for measuring picture similarity. It is being utilized in various types of applications, such as picture retrieval and matching [10], face authentication [11], and object identification.

Deep CNN need an input image with a constant size, such as 224 × 224 pixels. The image size is typically changeable rather than constant in real life. Some information in the picture may be lost if it is cropped or scaled to a specific size, which will lower the identification accuracy. A Spatial Pyramid Pooling (SPP) layer [12] was introduced to get around the network's fixed-size constraint and go beyond the limitation that CNN can only take pictures of a specific size. To be more precise, an SPP layer is added after the last convolutional layer, followed by completely connected layers. A CNN with an SPP layer may thus take images of any size and generate outputs of a specific dimension. This technique has been frequently used in recent years for object detection and image categorization [13].

This research uses a Siamese Neural Network (SNN) with subnetworks of identical architecture and parameter weights. Gene name images, with similar (anchor and positive samples) and unrelated images for other genes (negative examples) are used to train the deep learning model. The goal is for the model to develop the ability to assess visual similarity. This work examines a method for training SNNs that leverages a special topology to rank the similarity of inputs. We used a triple loss function that can reliably identify situations in which the distance between images in different classes is higher than the distance between images belonging to the same class, as shown in Fig. 1. When the training dataset is limited, such a triple loss

Muhammad Azam, Micheal Olaolu Arowolo, and Dong Xu are with Department of Electrical Engineering and Computer Science, University of Missouri, Columbia Missouri, USA (e-mail: moacvf@missouri.edu, matf8@missouri.edu, xudong@missouri.edu).

Fei He is with College of Information Science and Technology, Northeast Normal University, Changchun, Changchun, China (e-mail: hef740@nenu.edu.cn).

Mihail Popescu is with Department of Health Management and Informatics, University of Missouri, Columbia, Missouri, USA (e-mail: popescum@health.missouri.edu).

function may accelerate the convergence of the model learning. We adapted a triplet spatial pyramid pooling network (TSPP-Net) to combine the triplet convolution neural network with the SPP technique. No scaling or clipping is required for this network to accommodate any size of gene name images.

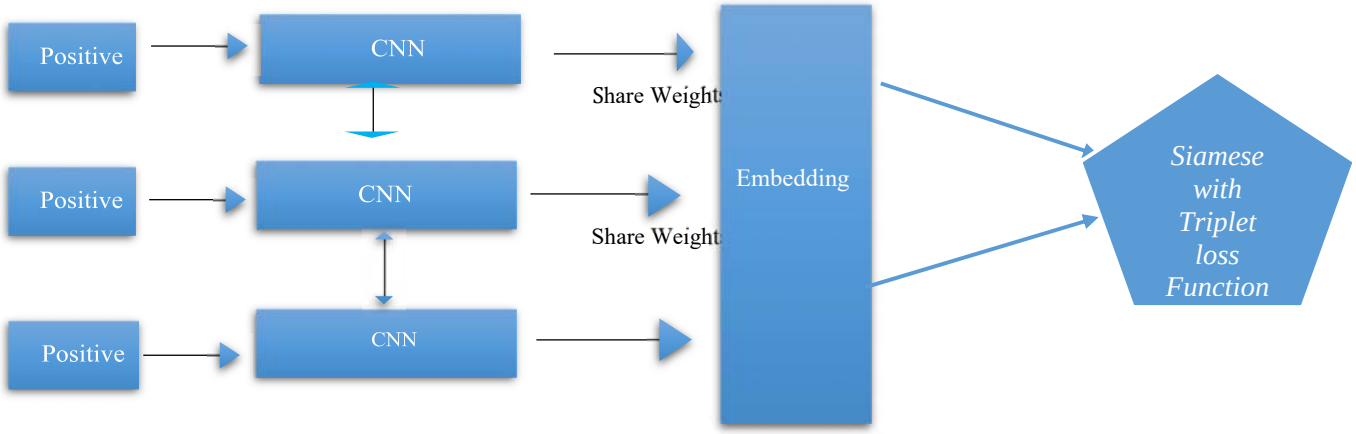

Fig. 1 Siamese triplet loss architecture for the model [14]

The remainder of this research paper is divided into the following sections: Section II discusses related work. The methods are presented in Section III. The results of our study are discussed in Section IV. Our conclusions and suggested future study areas are summarized in Section V.

II. Related Works

A foundation for pathway figure annotation is provided by gene name identifications from pathway figures [15], which might be helpful for updating pathway databases like KEGG [16]. Genes and their interactions may be identified using text and graphic representations of biomedical pathways [17]. Manual curation techniques cannot keep up with the expansion of the literature. To use route photos and text to uncover gene relationships, novel bio-curation techniques are required. Reference [10] suggests a route curation strategy using images and text from biology articles. To identify genes and their interactions from photos of pathways, it integrated deep learning object identification techniques with Google's OCR [18]. The process was evaluated using manually annotated PubMed figures. From route diagrams, the model successfully reconstructed genes and interactions. These biological curations might provide more knowledge-based resources and assist in developing biological techniques from the scientific literature.

Another strategy for finding genes in published pathway diagrams was proposed using OCR and route modeling [19]. The approach was optimized on PubMed Central figure images and tested against 400 curated Wike Pathways paths. The study found 29,189 gene symbols from 3982 published route diagrams over four years. This sampling of published numbers reveals new and diverse pathway relationships. The technique increased the number of genes associated with papers containing these statistics compared to PubMed and PubTator's combined annotations. In a separate study, 25 years' worth of pathway diagrams were analyzed for their troves of pathways knowledge [20]. More than a thousand genes were included here that were not in any other pathway databases.

Different from the previous work, our research does not use OCR but uses an SNN instead to identify gene identity names based on visual similarity. This work examines a method for training SNNs that leverages a special topology to naturally rank the similarity of inputs.

III. Materials and Methods

The Siamese network and enhanced triplet network are introduced in this section. The paper outlines an upgraded triplet network's structure (TSPP-Net) and the triplet loss function. The model was trained using backpropagation and mini-batch gradient descent.

A. Dataset

Since there was no publicly available pathway curation benchmark dataset, we created our own to train our object detection models on real-world data. Using several route-related keywords, we were able to extract images of 1095 genes, with a total of 4,121 text slice images of genes extracted from actual route diagrams using an existing tool [9]. As shown in Fig. 2, the genes are split into 825 for training and 102 for testing. Taking a cue from the face recognition process, this study employs a pre-trained VGGNet model to extract feature maps from the gene slices and then uses an SNN to fine-tune the model for recognizing gene names from pathway figures [13].

B. Siamese Network and Triplet Function

The Siamese network [21] maximizes the distance between the characteristics in two gene name images to determine how similar they are. Two identical CNN branches that share parameters (weights) make up the Siamese network. There is no final classification layer in a deep CNN; therefore, each branch is incomplete. The Siamese network derives an embedding feature, which is embodied by the function F, from each pair of

pictures. Equation (1) shows the contrastive loss function (L) given the inputs of the pictures X1 and X2, and a loss function between them D(X1,X2) = [F(X1)-F(X2)]^2:

$$L(X1, X2; m) = \frac{1}{2} . Y. D(X1, X2) + \frac{1}{2}. (1 - Y). \max(0, m - D(X1, X2)) \quad (1)$$

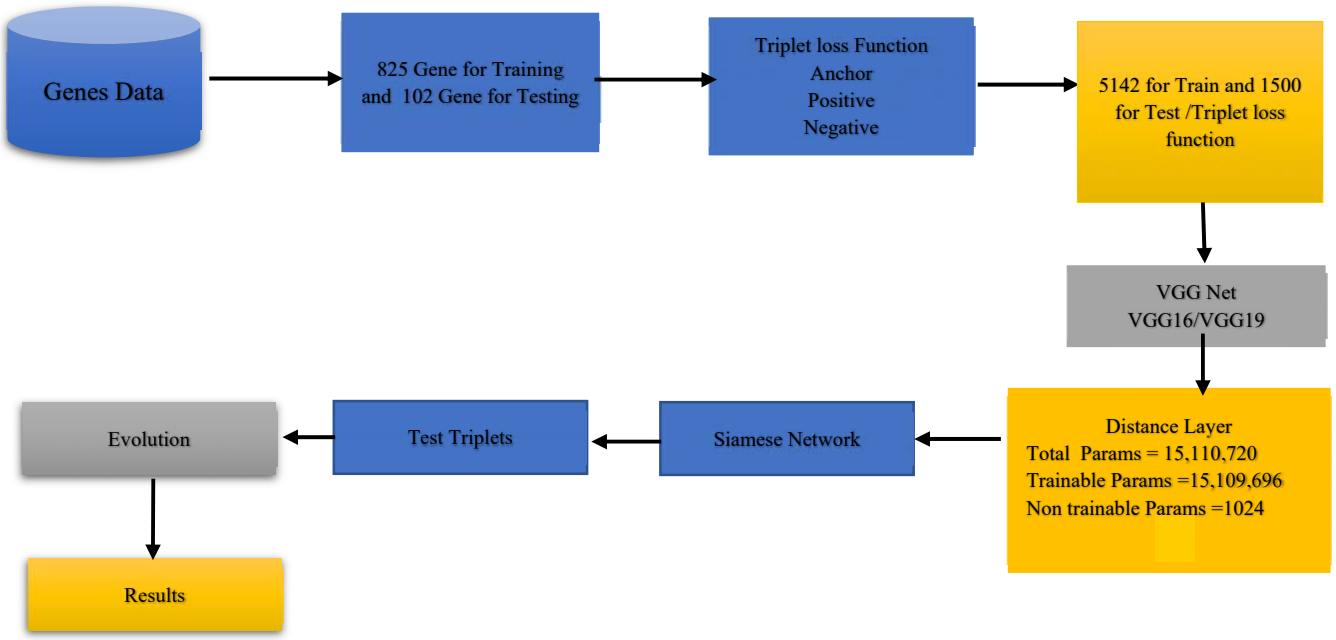

Fig. 2 Overview of the proposed workflow

where Y is a binary label for the input pictures X1 and X2. Y = 0 denotes dissimilarity or a negative value, whereas Y = 1 denotes similarity or a positive value. The threshold between positive and negative readings is represented by the parameter *m*. The ultimate objective is to discover new ideal network parameters and minimize the loss function using the training dataset.

The triple network model [4] was introduced to train a ranking function for image retrieval. It was used in Facial Net for face recognition and grouping [11]. Three pictures must be entered simultaneously for the triplet network: an anchor image (x^a), a positive image (x^p), and a negative image (x^n). The image pairs x^a and x^p are similar or are in the same category. The images x^a and x^n are in different categories or types of pictures. The system model creates a triplet contrastive loss function (L) based on the connection between the distances of three gene name pictures, as shown by (2):

$$L\left(x_i^a, x_i^p, x^n; \alpha\right) = \frac{1}{N} \sum_1^N max\ \{D\left(x_i^a, x_i^p\right) - D(x_i^a, x_i^n) + \alpha, 0\} \quad (2)$$

N indicates the number of triplet samples. The margin level refers to the difference between the distances, denoted as D, among the anchor and positive samples $D(x_i^a, x_i^p)$ and $D(x_i^a, x_i^n)$ the anchor and negative samples. The variables a, p, and n refer to anchor, positive, and negative samples, respectively, within a triplet.

The positive picture and the anchor image need to be separated from each other more than the negative image and anchor image are. A distance link exists for each triplet in the training dataset, as shown in (3):

$$D(x_i^a, x_i^p) + \alpha < D(x_i^a, x_i^n) \quad (3)$$

where α is a required buffer between pairings that are positive and negative. The square of the Euclidean distance is represented by D(.).

1. Spatial Pyramid Pooling

For deep CNN, the size of the input image is fixed (e.g., 224 224). Convolutional layers in CNN are not size-dependent and may build feature maps for images of any size. On the other hand, fully associated layers require inputs with predetermined lengths and sizes. In other words, the network's fixed-size restriction is only imposed by layers with perfect connections. To address this issue, Fig. 3 shows the addition of a SPP layer above the final convolutional layer [10]. The SPP layer collects the picture features from the feature map using the 4X4, 2X2, and 1X1 square grids. The SPP layer then generates 21 = 16 + 4 + 1 unique spatial bins and combines each block to provide an output of a defined size. Any feature map may generate a 5376-dimensional feature vector after SPP, where 5376 = 21X256. The fully linked layers receive the outputs of a fixed length that the SPP layer produces after combining the characteristics. The CNN with a SPP layer can handle pictures of any size and output a vector of a fixed size, leading to a considerable gain in precision without cropping or distorting the image.

$$D(x_i^a, x_i^p) + \alpha < D(x_i^a, x_i^n);\ D(x_i^a, x_i^p) + \beta < D(x_i^a, x_i^n) \quad (4)$$

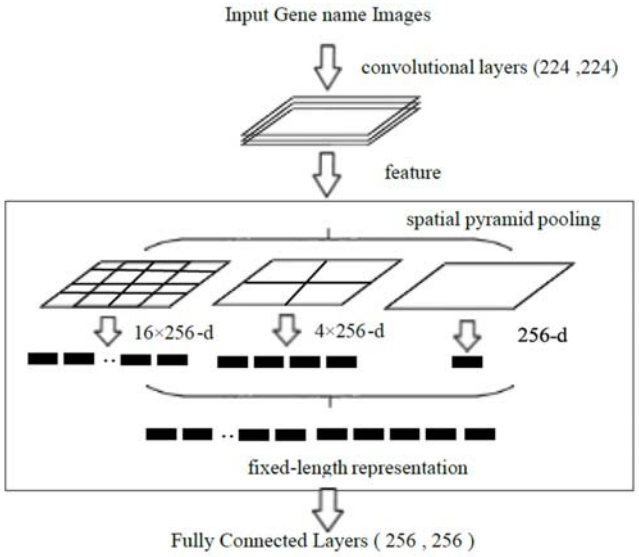

Fig. 3 The SPP layer for the gene names' identity

2. Improved Triplet Network

The Siamese and triplet networks can only process images of a certain size since they are built from two or three CNN branches, respectively. The TSPP-Net, which combines the SPP with the triplet network, is presented as a solution to this problem. There are also three identical CNN branches that share weights in the TSPP-Net. As seen in Fig. 3, a CNN may circumvent the disadvantages of fixed-size input images by adding a SPP layer above the final convolutional layer. This model requires an anchor image (x^a), a positive image (x^p), and a negative image (x^n), much like the triple network [18] does. In contrast to x^a and x^n, which are two pictures in two separate categories, x^a and x^p are two similar photographs in the same category. Fig. 4 shows a revised learning objective to enhance the model learning. The new target decreases the distance between an anchor and a positive, increases the distance between an anchor and a negative, and increases the distance between a positive and a negative. Once the learning objective has been optimized, the distance between the anchor image and the positive image is greater than both the distance between the anchor image and the negative image and the distance between the positive image and the negative sample, as shown in (4). Consequently, intra-class distance is less than inter-class distance, where α is the separate boundary between $D(x^a, x^p)$ and $D(x^a, x^n)$. The factor β is the gap margin between $D(x^a, x^p)$ and $D(x^p, x^n)$.

Equation (1) shows that the unique triple loss function, together with the added distance learning goals, may be used to readily construct the enlarged triple loss. The enhanced triple loss function may quadruple the amount of distance learning that can be done with only a triple sample when compared to the original triple loss function, as shown in (5):

$$L\left(x_i^a, x_i^p, x^n; \alpha, \beta\right) = \frac{1}{N}\sum_{1}^{N} \max\ \{D\left(x_i^a, x_i^p\right) - \mathrm{D}\left(x_i^a, x_i^p\right) + \alpha, 0\ \}$$
$$\frac{1}{N}\sum_i^N \max\{D\left(x_i^p, x_i^a\right) - D\left(x_i^p, x_i^n\right) + \beta, 0\} \quad (5)$$

where N represents the quantity of triplet models.

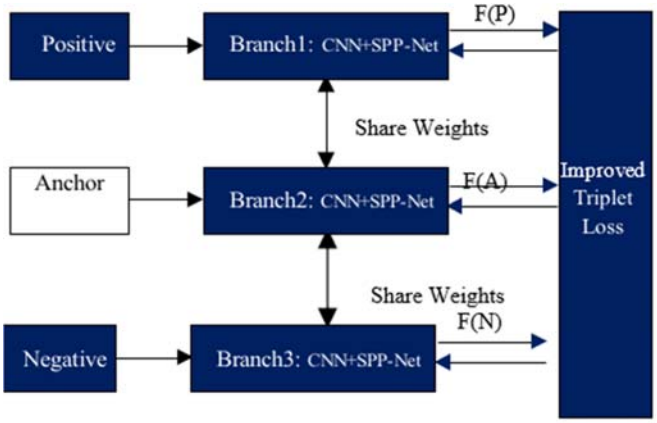

Fig. 4 TSPP-Net's construction

3. Siamese VGGNet

VGGNet is a widely used deep convolutional network [22] for object identification. VGG is an extension of Alex Net that increases the network's depth. Since the size of the whole convolution kernel is 3X3, the structure of VGG is clean and its topology is straightforward. The modest size of the convolution kernel provides benefits such as the ability to increase the number of layers. VGG increases the number of CNN layers to over ten, hence enhancing the expressive capacity of the network and simplifying later alterations to its structure.

VGGNet has shown considerable promise in research on picture categorization and object recognition. To combat gradient disappearance as network depth increases, VGGNet employs jump connections within its residual blocks [23]. Our network architecture consists of 50 layers, with each layer hiding between 128, 64, and 32 units. The activation function "relu" has been utilized for the input layer, the hidden layer, and the output layer. In total, 50 training epochs were used to optimize the model. We applied two VGG models in this work, VGG16 and VGG19. VGG16 is composed of convolution, reread, and pooling layers organized in a replicative structure, with a narrower receiving window for each convolutional filter than Alex Net [24]. VGG19 has a greater depth with extra convolutional readers in the array's midsection compared to VGG16, which improves the accuracy of the object identification [25].

4. Metrics of Assessment

The assessment criteria used to measure the success of the classification models used in this work following [26] include:

- Classification accuracy (CA): The ratio [27] of the number of accurate forecasts to the overall number of forecasts:

$$Accuracy = \frac{\mathrm{TP} + \mathrm{TN}}{\mathrm{TP} + \mathrm{TN} + \mathrm{FP} + \mathrm{FN}} \quad (6)$$

- Precision: The small percentage of the entire optimistic estimates which are accurately projected.

$$Percision = \frac{\mathrm{TP}}{\mathrm{TP} + \mathrm{FP}} \quad (7)$$

- Recall (sensitivity): The portion of all currently confirmed facts that were accurately estimated [27].

$$Recall = \frac{\text{TP}}{\text{TP + FN}} \quad (8)$$

- F-measure: The harmonic means of accuracy and recall. It shall be determined utilizing the method given as:

$$F - Score = \frac{2(\text{precision} * \text{Recall})}{(\text{percision} + \text{Recall})}$$

IV. Results and Discussions

We used the improved triple loss function with the SNN model in this work. This section shows the experiment's findings and an analysis of them.

A. Mean Average Precision

The trained network model for image retrieval allows us to extract features from images. Figs. 5 and 6 display the mean average precision (mAP) training and test evaluation image retrieval findings. All figures followed the same pattern. The average accuracy is VGG19 SNN < VGG16 SNN under the two multi-size training modes.

The improved triplet network and the Siamese network were both validated using the gene dataset. The two network models VGG16 and VGG19 were separately trained after which the relevant feature vectors were collected. We used the SNN approach to classify these vectors and compared the two models' classification accuracies while also examining the development of the margin values. Fig. 7 displays the outcomes. The Siamese VGG16 and the Siamese VGG19 networks both improved in classification accuracy when the number of epochs reached 50, 93%, and 92.94%, respectively.

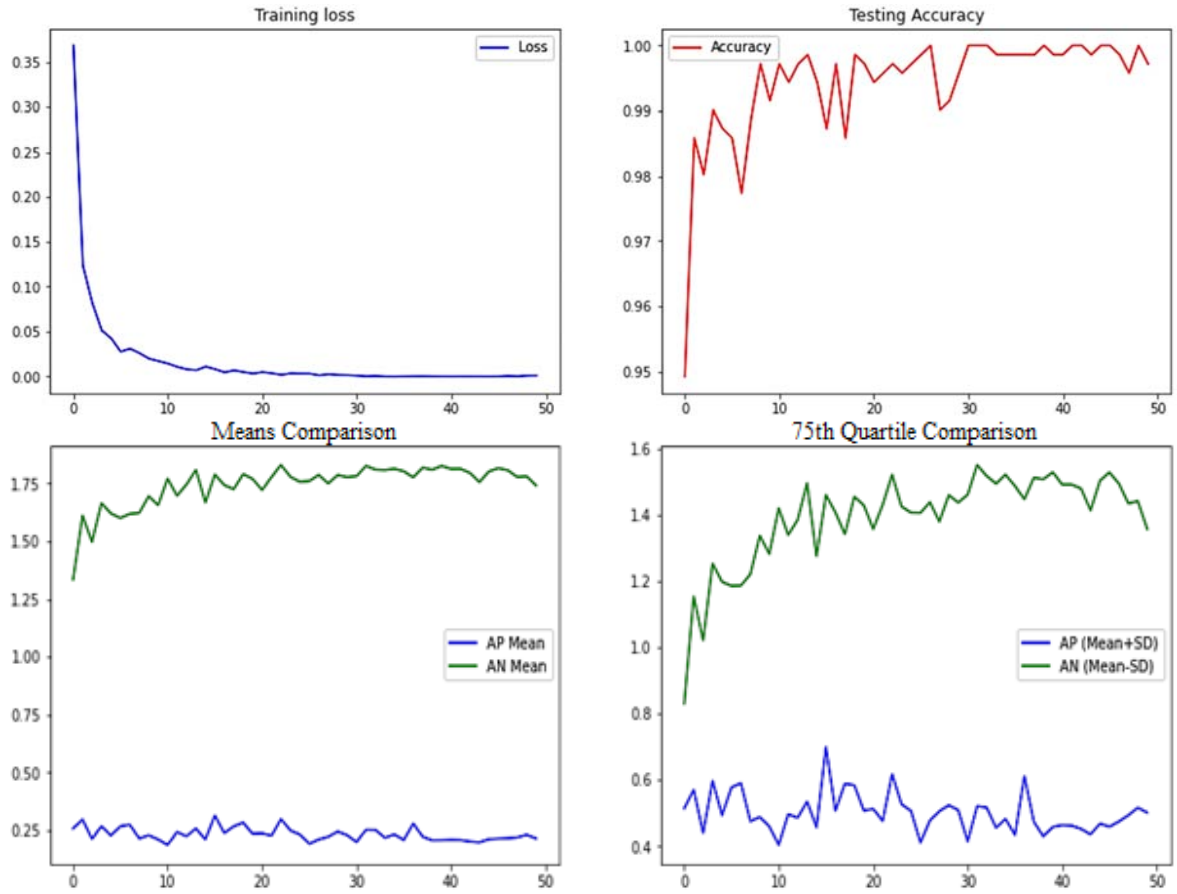

Fig. 5 Training and testing evaluations VGG16: The X-axis represents the list of epochs 0 to 50, and prediction accuracy has been presented by Y-axis

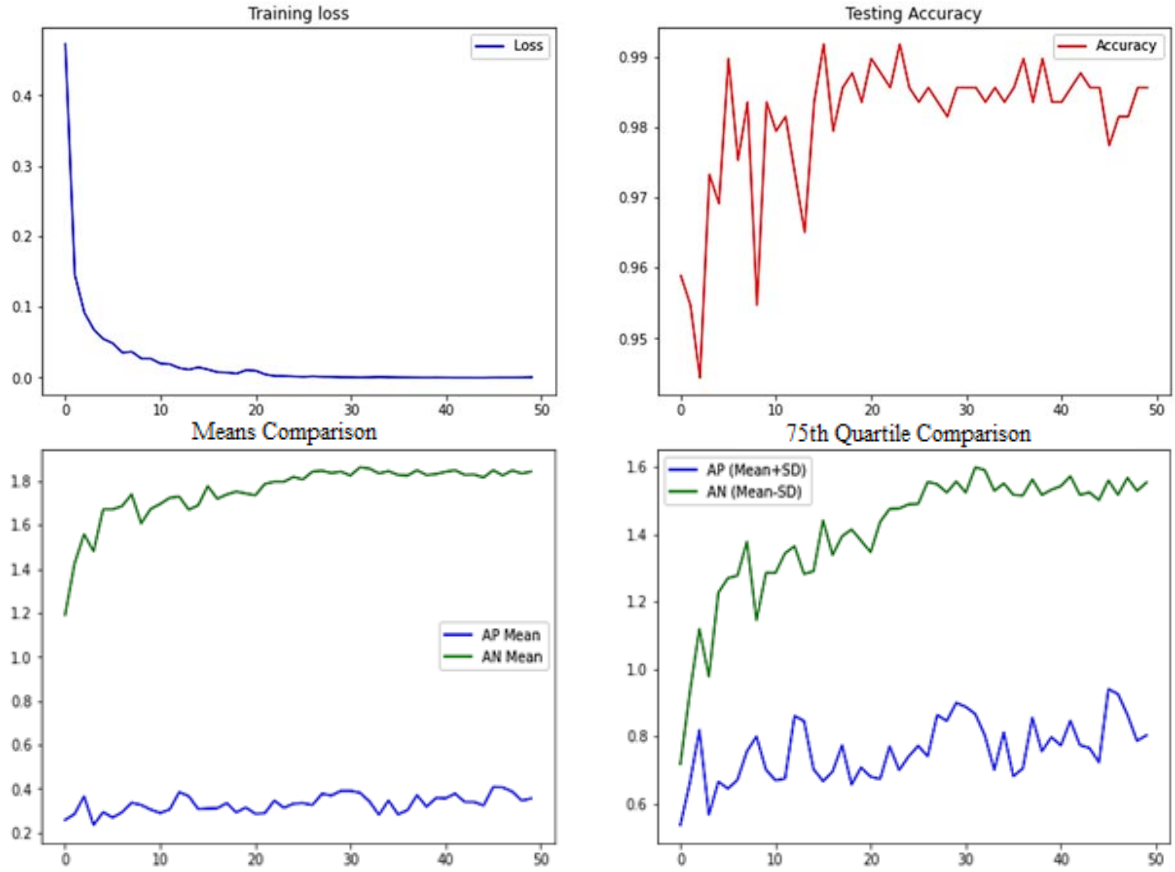

Fig. 6 Training and testing evaluations VGG19: The X-axis represents the list of epochs 0 to 50, and prediction accuracy has been presented by Y-axis

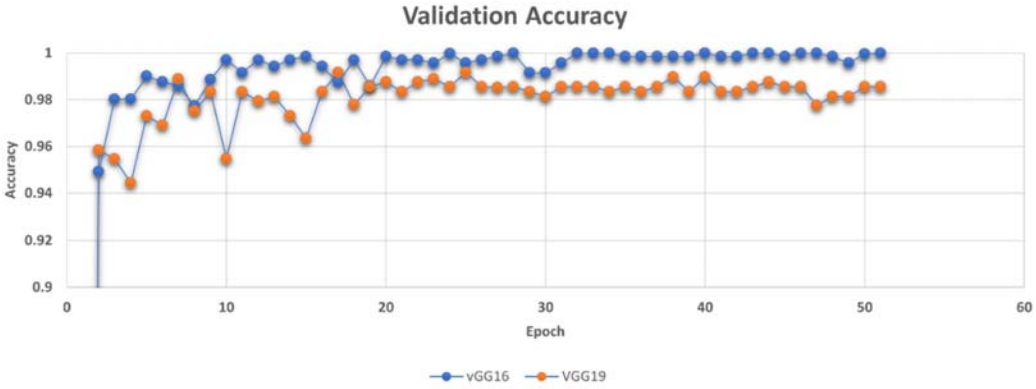

Fig. 7 Validation Results

Compared to the original triple network and the VGG 16 Siamese network, the upgraded and optimized VGG19 SNN network model has a higher classification accuracy. Fig. 8 displays the results of VGG16 and VGG19 using the described Siamese-VGGNet model. The model exhibits good accuracy in the datasets. The VGG16 Siamese network shows a higher accuracy of 93%, surpassing the VGG19 Siamese network, which achieves an accuracy of 92%. The precision score of VGG16 Siamese network is 97% and of VGG19 is 91%. To assess the model's effectiveness for gene recognition, we compared it to some recent OCR models, as shown in Table I. For the given cases, our proposed system outperforms other approaches like Tesseract Google OCR, and MMOCR in terms of performance.

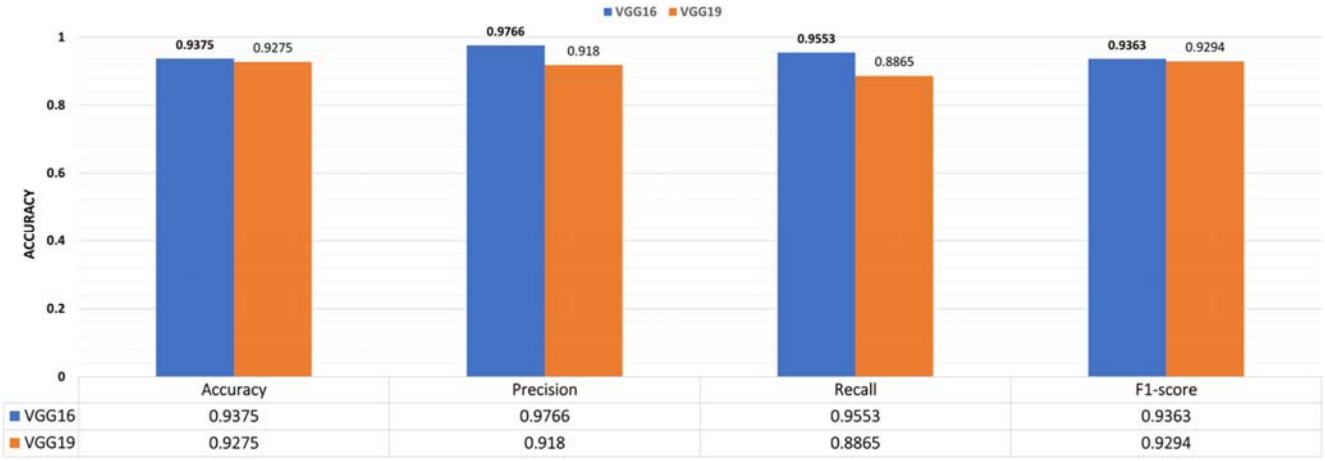

Fig. 8 Performance evaluation: The X-axis represents the Precision, Recall and F-1 measure, and prediction accuracy is presented by Y-axis from 0 to 1

TABLE I
COMPARISON WITH EXISTING SYNTHETIC IMAGES USING OCR FOR RECOGNITION [28]

Model	Accuracy
Google OCR	0.71
MM OCR	0.56
Easy OCR	0.34
Tesseract OCR	0.33
Kera's OCR	0.16
VGG16	0.9375
VGG19	0.9275

V. CONCLUSION

Automatically identifying essential genes and their roles from biological pathway figures can help retrieve biological knowledge in a large scale. Here, we offer a model that identifies genes from pathway figures accurately. Gene image retrieval using a Siamese model together with VGGNet was explored. Compared to image classification features, the features had better feature generalization and matching performance. It is necessary to use additional architectures to enhance the SNN model to prevent exhaustive feature map comparisons and enable online usage of the model distance layer. We may also attempt to train the network model in the future using multi-label learning or by combining the semantic information from the image to drastically decrease the computing time.

ACKNOWLEDGMENT

This study was made possible thanks to NIH funding number 5R01LM013392 from the National Library of Medicine. The writers alone are responsible for the material, which may not always reflect the National Institutes of Health's official positions.

REFERENCES

[1] D. Kim *et al.*, "A Neural Named Entity Recognition and Multi-Type Normalization Tool for Biomedical Text Mining," *IEEE Access*, vol. 7, pp. 73729–73740, 2019, doi: 10.1109/ACCESS.2019.2920708.

[2] C. Essien, F. He, M. Hannink, M. Popescu, and D. Xu, "Extraction of Gene Regulatory Relation Using Bio BERT," in *2022 IEEE International Conference on Bioinformatics and Biomedicine (BIBM)*, Las Vegas, NV, USA, Dec. 2022, pp. 3351–3355. Doi: 10.1109/BIBM55620.2022.9995458.

[3] J. Hu, J. Lu, and Y.-P. Tan, "Discriminative Deep Metric Learning for Face Verification in the Wild," in *2014 IEEE Conference on Computer Vision and Pattern Recognition*, Columbus, OH, USA, Jun. 2014, pp. 1875–1882. Doi: 10.1109/CVPR.2014.242.

[4] T. Bui, L. Ribeiro, M. Ponti, and J. Cellulose, "Compact descriptors for sketch-based image retrieval using a triplet loss convolutional neural network," *Compute. Vis. Image Underset.*, vol. 164, pp. 27–37, Nov. 2017, Doi: 10.1016/j.cviu.2017.06.007.

[5] S. Aldrich, M. O. Arowolo, F. He, M. Popescu, and D. Xu, "Comprehensive Assessment of OCR Tools for Gene Name Recognition in Biological Pathway Figures," in *2022 IEEE International Conference on Bioinformatics and Biomedicine (BIBM)*, Las Vegas, NV, USA, Dec. 2022, pp. 3574–3579. Doi: 10.1109/BIBM55620.2022.9995448.

[6] C. Szeged *et al.*, "Going deeper with convolutions," in *2015 IEEE Conference on Computer Vision and Pattern Recognition (CVPR)*, Boston, MA, USA, Jun. 2015, pp. 1–9. Doi: 10.1109/CVPR.2015.7298594.

[7] N. M. Asemia and P. D. D. Dominic, "Hyperparameter Optimization in Convolutional Neural Network using Genetic Algorithms," *Int. J. Adv. Compute. Sci. Appl.*, vol. 10, no. 6, 2019, Doi: 10.14569/IJACSA.2019.0100638.

[8] K. Simonyan and A. Zisserman, "Very Deep Convolutional Networks for Large-Scale Image Recognition." arXiv, Apr. 10, 2015. Accessed: Dec. 18, 2022. (Online). Available: http://arxiv.org/abs/1409.1556

[9] E. Hoffer and N. Alon, "Deep metric learning using Triplet network." arXiv, Dec. 04, 2018. Accessed: Nov. 21, 2022. [Online]. Available: http://arxiv.org/abs/1412.6622

[10] S. Apparatus, "Image similarity using Deep CNN and Curriculum Learning," p. 9.

[11] F. Shroff, D. Maleficence, and J. Philbin, "Face Net: A unified embedding for face recognition and clustering," in *2015 IEEE Conference on Computer Vision and Pattern Recognition (CVPR)*, Boston, MA, USA, Jun. 2015, pp. 815–823. Doi: 10.1109/CVPR.2015.7298682.

[12] Y. Cao, C. Lu, X. Lu, and X. Xia, "A Spatial Pyramid Pooling Convolutional Neural Network for Smoky Vehicle Detection," in *2018 37th Chinese Control Conference (CCC)*, Wuhan, Jul. 2018, pp. 9170–9175. Doi: 10.23919/ChiCC.2018.8483521.

[13] C.-Q. Huang, S.-M. Yang, Y. Pan, and H.-J. Lai, "Object-Location-Aware Hashing for Multi-Label Image Retrieval via Automatic Mask Learning," *IEEE Trans. Image Process.*, vol. 27, no. 9, pp. 4490–4502, Sep. 2018, Doi: 10.1109/TIP.2018.2839522.

[14] E. Jahan Heave, H. Habibi Agama, and D. Puig, "An optimized convolutional neural network with bottleneck and spatial pyramid pooling layers for classification of foods," *Pattern Recognin. Lett.*, vol. 105, pp. 50–58, Apr. 2018, doi: 10.1016/j.patrec.2017.12.007.

[15] F. He, D. Wang, Y. Innocentia, O. Kholod, D. Shin, and D. Xu, "Extracting Molecular Entities and Their Interactions from Pathway

Figures Based on Deep Learning," in *Proceedings of the 10th ACM International Conference on Bioinformatics, Computational Biology and Health Informatics*, Niagara Falls NY USA, Sep. 2019, pp. 397–404. Doi: 10.1145/3307339.3342187.

[16] M. Kunihisa, M. Furuuchi, M. Tanabe, Y. Sato, and K. Mishima, "KEGG: new perspectives on genomes, pathways, diseases and drugs," *Nucleic Acids Res.*, vol. 45, no. D1, pp. D353–D361, Jan. 2017, Doi: 10.1093/Nar/gkw1092.

[17] K. Hanapers, A. Riitta, M. Summer-Kitman, and A. R. Pico, "Pathway information extracted from 25 years of pathway figures," *Genome Biol.*, vol. 21, no. 1, p. 273, Dec. 2020, doi: 10.1186/s13059-020-02181-2.

[18] X. Liu, M. Liu, L. Dong, M. Hui, Y. Zhao, and L. Peng, "SAR target recognition and posture estimation using spatial pyramid pooling within CNN," in *2017 International Conference on Optical Instruments and Technology: Optoelectronic Imaging/Spectroscopy and Signal Processing Technology*, Beijing, China, Jan. 2018, p. 27. doi: 10.1117/12.2285913.

[19] K. He, X. Zhang, S. Ren, and J. Sun, "Spatial Pyramid Pooling in Deep Convolutional Networks for Visual Recognition," *IEEE Trans. Pattern Anal. Mach. Intel.*, vol. 37, no. 9, pp. 1904–1916, Sep. 2015, Doi: 10.1109/TPAMI.2015.2389824.

[20] M. Kim, S. H. Beak, and M. Song, "Relation extraction for biological pathway construction using node2vec," *BMC Bioinformatics*, vol. 19, no. S8, p. 206, Jun. 2018, doi: 10.1186/s12859-018-2200-8.

[21] I. Malakhov, J. Kanaloa, and E. Rathi, "Siamese network features for image matching," in *2016 23rd International Conference on Pattern Recognition (ICPR)*, Cancun, Dec. 2016, pp. 378–383. Doi: 10.1109/ICPR.2016.7899663.

[22] H. Key, D. Chen, X. Li, Y. Tang, T. Shah, and R. Ranjan, "Towards Brain Big Data Classification: Epileptic EEG Identification with a Lightweight VGGNet on Global MIC," *IEEE Access*, vol. 6, pp. 14722–14733, 2018, Doi: 10.1109/ACCESS.2018.2810882.

[23] Q. Yu, Y. Xu, J. Liu, Z. Xi, Z. Li, and Y. Liu, "Fibronectin Promotes the Malignancy of Glioma Stem-Like Cells Via Modulation of Cell Adhesion, Differentiation, Proliferation and Chemoresistance," *Front. Mol. Neurosis.*, vol. 11, p. 130, Apr. 2018, Doi: 10.3389/fnmol.2018.00130.

[24] F. N. Bandola, S. Han, M. W. Moszkowicz, K. Ashraf, W. J. Dally, and K. Kreutzer, "Squeeze Net: Alex Net-level accuracy with 50x fewer parameters and <0.5MB model size." arXiv, Nov. 04, 2016. Accessed: Dec. 18, 2022. (Online)s. Available: http://arxiv.org/abs/1602.07360

[25] J. Zhou and B. Fu, "The research on gene-disease association based on text-mining of PubMed," *BMC Bioinformatics*, vol. 19, no. 1, p. 37, Dec. 2018, Doi: 10.1186/s12859-018-2048-y.

[26] T. Kymani, T. Karas, S. Laine, J. Lehtonen, and T. Aila, "Improved Precision and Recall Metric for Assessing Generative Models".

[27] P. A. Marin-Reyes, L. Ber Gamini, J. Lorenzo-Navarro, A. Palazzi, S. Caldara, and R. Cochair, "Unsupervised Vehicle Re-identification Using Triplet Networks," in *2018 IEEE/CVF Conference on Computer Vision and Pattern Recognition Workshops (CVPRW)*, Salt Lake City, UT, USA, Jun. 2018, pp. 166–1665. doi: 10.1109/CVPRW.2018.00030.

[28] S. Aldrich, M. Arowolo, F. He, M. Popescu, and D. Xu, "*Comprehensive Assessment of OCR Tools for Gene Name Recognition in Biological Pathway Figures," in 2022 IEEE International Conference on Bioinformatics and Biomedicine (BIBM)*, Las Vegas, NV, USA